ACS APPLIED MATERIALS & INTERFACES

Research Article

www.acsami.org

Massively Parallel Patterning of Complex 2D and 3D Functional Polymer Brushes by Polymer Pen Lithography

Zhuang Xie,[†,‡] Chaojian Chen,[‡] Xuechang Zhou,[†,‡] Tingting Gao,[‡] Danqing Liu,[§] Qian Miao,[§] and Zijian Zheng*[,†,‡]

[†]The Hong Kong Polytechnic University Shenzhen Research Institute, Shenzhen, China

[‡]Nanotechnology Center, Institute of Textiles and Clothing, The Hong Kong Polytechnic University, Hong Kong SAR, China

[§]Department of Chemistry, The Chinese University of Hong Kong, Hong Kong SAR, China

Supporting Information

ABSTRACT: We report the first demonstration of centimeter-area serial patterning of complex 2D and 3D functional polymer brushes by high-throughput polymer pen lithography. Arbitrary 2D and 3D structures of poly(glycidyl methacrylate) (PGMA) brushes are fabricated over areas as large as 2 cm × 1 cm, with a remarkable throughput being 3 orders of magnitudes higher than the state-of-the-arts. Patterned PGMA brushes are further employed as resist for fabricating Au micro/nanostructures and hard molds for the subsequent replica molding of soft stamps. On the other hand, these 2D and 3D PGMA brushes are also utilized as robust and versatile platforms for the immobilization of bioactive molecules to form 2D and 3D patterned DNA oligonucleotide and protein chips. Therefore, this low-cost, yet high-throughput "bench-top" serial fabrication method can be readily applied to a wide range of fields including micro/nanofabrication, optics and electronics, smart surfaces, and biorelated studies.

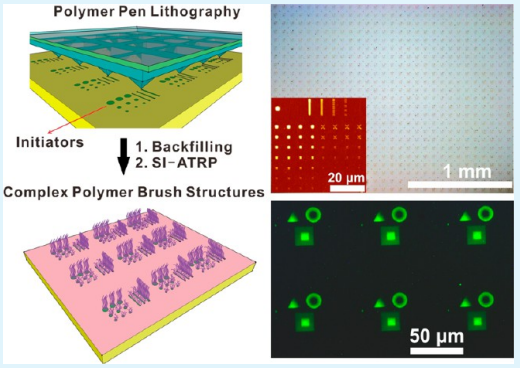

KEYWORDS: *polymer pen lithography, polymer brushes, three-dimensional structures, micro/nanofabrication, biomolecular array*

1. INTRODUCTION

Engineering surfaces with functional polymers is a crucial issue in a wide range of research fields from micro/nanofabrication and biomimetic and smart surfaces to cell-material interface studies.[1−5] In particular, polymer brushes have shown remarkable advantages over traditional spin-casted films for surface functionalization because the vertically aligned, surface-tethered polymer chains create a robust three-dimensional (3D) environment with high spatial density of functional groups,[6,7] which are desirable for high-capacity immobilization of biomolecules,[8−11] nonfouling surfaces,[12,13] controlled assembly of ionic species and nanomaterials,[14,15] and stimuli-responsive smart surfaces.[2,16−18] The ability to pattern polymer brushes further extends their applications into new areas such as micro/nanofluidic devices, sensors and actuators, bioassays for diagnostics, templates for cell growth and differentiation, as well as the fundamental study of the polymer behavior at different length scales.[19−23] Recently, beyond two-dimensional (2D) arrays, polymer brushes have also been employed to construct 3D gradient or complex 3D structures, which are particularly highlighted in material and biorelated researches for the studies in cell adhesion and growth, surface molecular transport or high-throughput screening of nanomaterials.[7,24]

Despite the tremendous potentials of complex 2D and 3D polymer brush structures, the lack of high-throughput tools to fabricate them over a macroscopic area has dramatically hindered their usage both in fundamental research and practical applications. Current serial lithographic methods such as e-beam lithography (EBL)[25−28] and scanning probe lithography (SPL)[12,29−35] are dominant techniques in fabricating complex 2D and 3D polymer brushes with ultrahigh resolution. The fatal drawback for the serial methods, however, is very low throughput, leading to limited patterning areas and very high cost per patterning unit. Indeed, the state-of-the-art demonstration of patterning 2D and 3D arrays of polymer brushes by serial methods is limited to a throughput of ∼1 mm × 0.1 mm in 1 h, far too low for most applications. On the other hand, mask or mold-based lithography such as photolithography,[36−39] imprint lithography,[40,41] colloidal lithography,[22] and microcontact printing[42−45] can rapidly produce patterned polymer brushes with submicrometer resolution over square-centimeter areas. Nevertheless, it is challenging for these approaches to produce arbitrary and complex structures with fine control, despite a few reports on the patterning of gradient polymer brushes by varying the optical intensity[36−38] or by multistep contact printing.[42−44] To date, how to realize large-area fabrication of complex 2D and 3D polymer brushes for

Received: December 4, 2013
Accepted: January 13, 2014
Published: January 13, 2014

 © 2014 American Chemical Society

practical applications in a simple, rapid, and cost-effective manner remains to be a central challenge in this field.

In this paper, we report a "bench-top" printing method that allows massively parallel and serial patterning of 2D and 3D polymer brushes over macroscopically large areas, and its applications in material micro/nanofabrication and microarray-based bioassays. This method makes use of a recently developed technique named polymer pen lithography (PPL)[46] to print initiator molecules on a substrate followed by growth of functional polymer brushes via surface-initiated atom transfer radical polymerization (SI-ATRP, Scheme 1).

Scheme 1. Schematic Illustration of the Large-Area, Arbitrary Patterning of PGMA Brushes through PPL and SI-ATRP

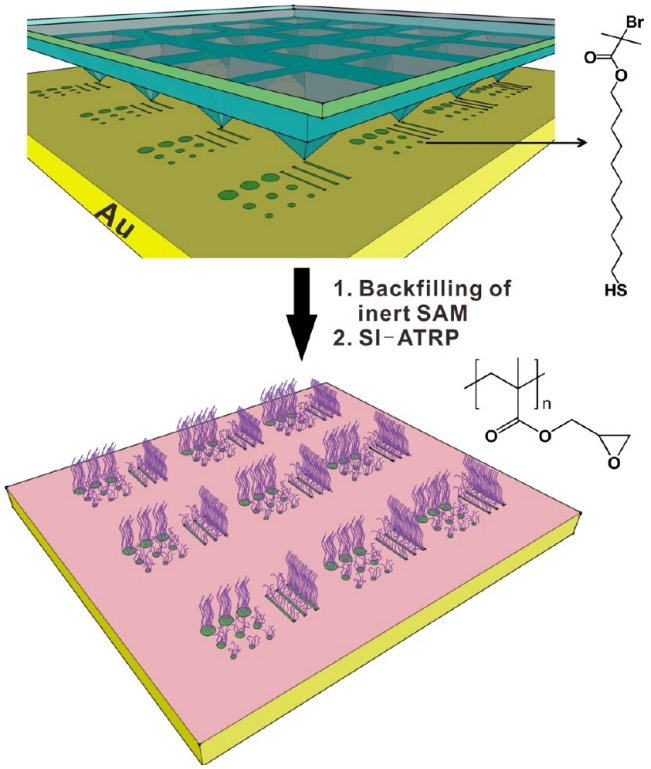

PPL is a scanning-probe-based printing technique, which utilizes a low-cost elastomeric tip array containing as many as 10^7 tips to directly write ink materials onto the substrate under the control of piezoelectric actuators of an atomic force microscope (AFM).[46−50] We show that patterned submicrometer-sized 2D arrays and complex 3D arrays of polymer brushes can be readily generated by this low-cost printing method over square-centimeter areas with good uniformity, and more importantly, a remarkable throughput being 3 orders of magnitudes higher than the best result reported in the literatures using serial fabrication methods. This method can meet the throughput and resolution requirement for lab-scale rapid prototyping of functional 2D and 3D templates for various purposes. As proof-of-concept, we demonstrate the use of 2D arrays of polymer brushes as effective etching resist for micro/nanofabrication of hard molds and soft stamps, and 3D-patterned polymer brushes as functional templates to generate bioactive DNA and protein 3D arrays.

2. EXPERIMENTAL SECTION

Materials. The ATRP initiator ω-mercaptoundecyl bromoisobutyrate (MUDBr) was kindly provided by Prof. Hongwei Ma, Suzhou Institute of Nano-Tech and Nano-Bionics. Oligonucleotides were purchased from Takara (Dalian, China). The target sequence was 5′-NH_2-$(CH_2)_6$-CAT GAT TGA ACC ATC CAC CA-TET-3′ and the probe sequence was 5′-TAMRA-TGG TGG ATG GTT CAA TCA TG-3′. The random control sequence was 5′-TAMRA-CAT AGT GTG GAC CCC TAG CA-3′. Glycidyl methacrylate (GMA, Aldrich) was purified on a neutral alumina column before use. All other chemicals were obtained from Sigma-Aldrich and used as received. Au substrates were prepared by thermal evaporation of 25 nm Au/5 nm Cr on n-doped ⟨100⟩ silicon wafers.

Fabrication of Polymer Pen Arrays. A silicon mold with recessed pyramid microwells was fabricated by standard photolithography and wet etching following previously reported procedures.[47] Hard polydimethylsiloxane (*h*-PDMS) precursors consisting of vinyl-compound-rich prepolymer (VDT-731, Gelest) and hydrosilane-rich cross-linker (HMS-301) were mixed at a ratio of 3.4:1 by weight. The mixture was degassed under vacuum and poured on top of the silicon mold. A piece of plasma-treated glass slide was placed to cover the precursor as support. The whole assembly was cured at 80 °C overnight, and then, the solidified polymer pen array with glass support was carefully separated from the mold.

Polymer Pen Lithography. Prior to patterning, the Au substrates were cleaned by ultrasonication in DI water, acetone, and isopropanol, sequentially, and were blown dry with N_2. A drop of 1 mM ω-mercaptoundecyl bromoisobutyrate (MUDBr) ethanol solution was spin coated onto the polymer pen array at 3000 rpm for 30 s for inking. The inked polymer pen array was then mounted onto the customer-made z-piezo scanner (XE-100, Park Systems) and aligned to the plane of the Au substrate. After leveling, the pen array was programmed to contact with the substrate to write the initiator patterns at 15−20% relative humidity and room temperature (RT). Finally, the initiator-patterned substrate was backfilled with 1 mM octadecylthiol (ODT) or 0.5 mM 11-mercaptoundecyl tri(ethylene glycol) (EG_3) ethanol solution for 30 min.

SI-ATRP of PGMA Brushes. GMA (7.5 mL), methanol (6 mL) and DI water (1.5 mL) were mixed and bubbled with argon for 15 min in a Schlenk tube, followed by dissolving copper(I) bromide (CuBr, 78 mg) and 2,2′-dipyridyl (dipy, 210 mg). The resulting dark brown mixture was transferred into an argon purged 15 mL centrifuge tube containing the initiator-patterned substrate to start the polymerization. After 2 h polymerization at 30 ± 1 °C, the substrate was taken out and rinsed with methanol and water; then, it was washed in dichloromethane and methanol, followed by blow drying with compressed air.

Au Etching and PDMS Stamp Fabrication. The patterned PGMA brushes were exposed to 30 s O_2 plasma to remove the background SAM. Subsequently, the substrate was immersed in the Au etching solution containing 2 mM thiourea, 30 mM $Fe(NO_3)_3$, 20 mM HCl and 20 mM octanol for 5 min to obtain the Au patterns. To transfer the pattern to a PDMS stamp, a thin layer of 10 nm Au/2 nm Cr was evaporated onto the etched substrate. Subsequently, the substrate was immersed in 5 mM 1H,1H,2H,2H-perfluorodecanethiol ethanol solution for 24 h. PDMS (Sylgard 184, Dow Corning) prepolymer and cross-linker (10: 1 w/w) were mixed and degassed, and then the liquid was poured onto the fluoro-treated substrate and cured at 70 °C for 2 h to obtain PDMS stamp with replicated patterns.

Immobilization of Biomolecules. The substrate with patterned PGMA brushes and EG_3 background was employed in the immobilization experiments. A 20-mer, 5′-amine-modified oligonucleotide labeled with TET in 3′position was dissolved in 1× PBS (pH = 8) to prepare a 10 μM solution. The substrate was covered with the target oligonucleotide solution (ca. 10 μL) and then placed in a sealed chamber with saturated NaCl solution overnight at RT. Unreacted oligonucleotides were removed by washing with 1× PBS and DI water under vigorous shaking for 15 min. Subsequently, the reactive groups on the substrate were blocked with 50 mM ethanolamine in 10× Tris EDTA (pH = 7.6) for 1.5 h at RT. For hybridization, 100 nM

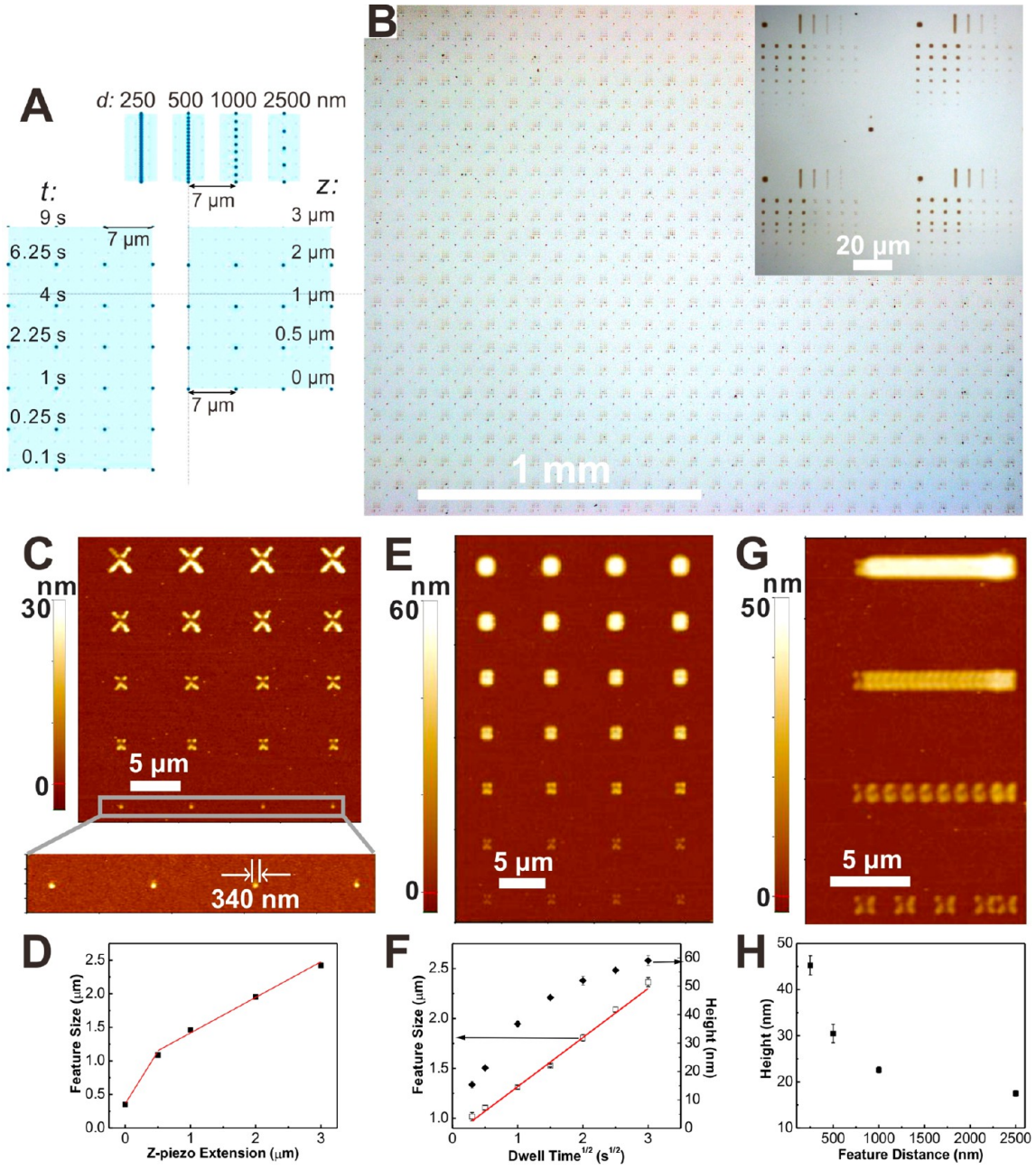

Figure 1. (A) Designed patterning parameters for brush arrays in PPL. In the bottom left array, the dwell time (t) ranges from 0.1 to 9 s from bottom to top, and the z-piezo extension (z) is set as 0.5 μm; in the bottom right array, z increases from 0 to 3 μm from bottom to top (t = 0.25 s); in the top array, the feature distance (d) varies from 250 to 2500 nm from left to right, with t = 0.25 s and z = 0.5 μm. (B) Optical microscope images of the patterned PGMA brush arrays over large areas. (C) AFM topography of a typical PGMA brush array made with various z-piezo extensions. (D) Plot of the feature size versus z-piezo extension. (E) AFM topography of PGMA brush array made with various dwell times. (F) Plot of the feature size and brush height versus $t^{1/2}$. (G) AFM topography of PGMA brush array made with various feature distances. (H) Statistical results of the brush height at different feature distance, obtained from four different arrays.

TAMRA-labeled oligonucleotide in the hybridization buffer (4× SSC, 0.08% SDS) was applied to the above substrate. The hybridization was maintained at 45 °C for 7 h, followed by sequentially washing the substrate with hybridization buffer at 45 °C for 10 min, 0.1× SSC with 0.01% SDS for 5 min at RT and DI water for 5 min. Protein immobilization was achieved by dropping 1 μL of IgG (from human serum, Sigma) solution (50 μg mL^{-1} in 1× PBS) onto the brush-patterned substrate. After 16 h incubation at RT, the substrate was washed in 0.6× PBS, 0.02% Tween-20 with vigorous agitation for 30 min. The substrate was blocked with BSA (100 μg mL^{-1} in 1× PBS) at 37 °C for 30 min and then was incubated with FITC-labeled anti-IgG (antihuman IgG-FITC antibody produced in goat, Sigma) solution (0.1−50 μg mL^{-1} in 1× PBS) at RT for 2 h, followed by thoroughly washing.

Characterization. Optical and fluorescent images were recorded with a Nikon Eclipse 80i optical microscope (Nikon, Japan), λ_{ex} = 465−495 nm, λ_{obs} = 515−555 nm for green fluorescence and λ_{ex} = 528−553 nm, λ_{obs} = 577−632 nm for orange fluorescence. AFM topography was measured by an XE-100 AFM (Park Systems, Korea) with noncontact mode at ambient conditions. ATR-FTIR was performed using PerkinElmer Spectrum 100 FI-TR spectrometer. SEM images were taken with a Hitachi TM3000 tabletop electron microscope (Hitachi High-Technologies Corp., Japan).

3. RESULTS AND DISCUSSION

Patterning of 2D and 3D Polymer Brush Arrays. Polymer pen arrays with pyramidal tips made of hard polydimethylsiloxane (*h*-PDMS) were used to conduct the PPL experiments (see Experimental Section for detail fabrication process of the pen arrays). In a typical experiment, the size of the tip array is 6.6 × 4.2 mm^2 and it contains ∼4500 pyramidal tips (40 μm edge length, 80 μm pitch) with tip radius of curvature being 100 nm. The polymer pen array was inked with the ATRP initiator ω-mercaptoundecyl bromoisobutyrate (MUDBr) by spin coating and then attached onto the customer-made scanning head (XE-100, Park Systems), which was placed in an environmental chamber (15%-20% relative humidity, 25 ± 1 °C). The inked tips were leveled and then brought to contact with the underlying Au substrate at different positions, dwell times, and contact areas, where MUDBr molecules diffused and self-assembled on the Au surfaces at the areas of contact. As shown in the design schematic in Figure 1A, each pyramidal tip was programmed to fabricate three arrays: a 7 × 4 dot array (pitch = 7 μm) with dwell time (t) ranging from 0.1 to 9 s in each column, a 5 × 4 dot array (pitch = 7 μm) with z-piezo extension (z) ranging from 0 to 3 μm in each column, and a dotted line array of 4 lines (pitch = 7 μm) with dot-to-dot distance (d) decreasing from 2500 to 250 nm in each line. After PPL patterning, the Au substrate was immediately backfilled with inert thiols such as octadecylthiol (ODT) or 11-mercaptoundecyl tri(ethylene glycol) (EG_3) for surface passivation. Multifunctional poly(glycidyl methacrylate) (PGMA) was chosen as the target polymer because its reactive epoxy side groups could be used for further immobilization of biomolecules. PGMA brushes were grown from the initiating moieties by immersing the MUDBr-patterned Au substrate into a polymerization solution. After brief rinsing with fresh solvents, patterned arrays of PGMA brushes were clearly seen from the optical microscope (Figure 1B), where the denser polymer brushes showed darker appearance. All tips of the pen array succeeded in patterning (Supporting Information (SI), Figure S1); that is, ∼4500 replicas of PGMA arrays were fabricated simultaneously in ∼20 min.

Because the tip arrays are fabricated by molding methods with PDMS similar to those in soft lithography, the size of the tip arrays and the number of tips can be readily scaled up. In the current study, we also succeeded in fabricating a larger tip array (2 cm × 1 cm) containing ∼3 × 10^4 tips, and using this tip array to fabricate similar PGMA structures following the same procedures (SI, Figure S2). Compared with the state-of-the-art parallel serial fabrication of polymer brushes in the literature, the throughput of our method is at least 3 orders of magnitudes higher. For example, patterning by single AFM tip[32] and 1D cantilever array[33] present a patterning speed of 1 and 18 features per writing time within an area of 0.1 × 0.1 mm^2 and 0.1 × 1.2 mm^2, respectively, while PPL shows at least 10^3 fold increase in speed (10^3–10^4 features per writing time) and covered area (>1 × 1 cm^2), despite the lower patterning resolution by polymer tip (∼300 nm) than that by Si tip (∼100 nm). Note that the throughput can even be improved much further, providing that larger tip and sample holders are used. Because of the considerable quantity of patterned brushes over a macroscopic area, we were able to verify the chemical structures of PGMA by attenuated total reflectance Fourier transform infrared (ATR-FTIR) spectroscopy. Indeed, characteristic peaks of GMA were found at 907 cm^{-1} for the epoxide group, 1265 and 1150 cm^{-1} for the ester group, 1735 cm^{-1} for the carbonyl group, and 2930 and 2855 cm^{-1} for C–H stretching (SI, Figure S3). In contrast, this kind of spectroscopic analysis of structures fabricated by low-throughput serial methods is very difficult because the patterning area is typically less than 1 mm^2.

Importantly, the feature size of PGMA brushes can be tailored by controlling the contact force and contact time in PPL experiments,[48] which allows rapid generation of patterns with size ranging from submicrometer to tens of micrometers and various shapes. At initial contact between the tip and the substrate (z-piezo extension = 0, t = 0.25 s), nanodots of PGMA brushes (∼340 nm edge size) were fabricated (Figure 1C, magnified image). When gradually pushing the z-piezo extension to 3 μm, that is, increasing the contact force between the tip and the substrate, the edge size of PGMA brushes increased to 2.42 ± 0.03 μm as a first-order function of the z-piezo extension (Figure 1C and D). The size change is attributed to the elastic deformation of the tips at different applied forces. Note that "X"-shaped features of polymer brushes were obtained at z > 0.5 μm instead of square ones, indicating an uneven distribution of the initiators on the tip–substrate contacts at large z-extensions. This phenomenon can be explained by the fact that, at short contact time and large contact area, the initiator molecules do not have enough time to fill the underlying substrate.

The insufficient deposition of ink can be addressed by increasing the dwell time. Indeed, we observed an obvious shape transition from "X" to square and to dot, when we gradually increased the dwell time from 0.1 to 9 s at fixed contact force (z = 0.5 μm). Notably, the shape transition was accompanied with size increase on both the edge length and height of the brushes: the edge length of PGMA features increased from 1.02 ± 0.04 μm to 2.36 ± 0.05 μm as a first-order function of $t^{1/2}$, and the corresponding brush height raised from 15 ± 1 nm to 59 ± 2 nm (Figure 1E and F). These phenomena can be ascribed to the diffusion of thiol initiators. As time goes, the initiator molecules can diffuse to fill in all the tip–substrate contact areas to form square shape. In the mean time, they also diffuse laterally through the water meniscus between the tip and the substrate so that the edge length grows. Since the lateral diffusion is isotropic, the square feature shall eventually become dot shape. During the ink diffusion process, the grafting density of initiator molecules, that is, number of initiator molecules per unit area, also increases. When polymer brushes grow from denser initiators, the polymer chains tend to stretch up to form a higher structure because of the stronger repulsion force between neighboring chains, and vice versa.

Apart from fabricating 2D arrays of polymer brushes, we also employ a "feature density" method we previously reported[32,33] to fabricate large-area 3D polymer structures. In the feature density method, polymer brushes of the same size and height are used as building blocks and are positioned in controlled lateral spacing. When the spacing is small enough, the topography of the neighboring building blocks will change because of the configuration stretching of the polymer chains. For instance, isolated PGMA brush dots with size of ∼1.2 μm and height of 17 ± 1 nm were fabricated at the dot-to-dot spacing of 2500 nm. As the feature spacing reduced to 250 nm, the brush dots were observed to merge together, accompanied with increase in the brush height. Finally, lines with smooth top surface were obtained at the 250-nm feature distance with the average brush height of 45 ± 2 nm (Figure 1G and H).

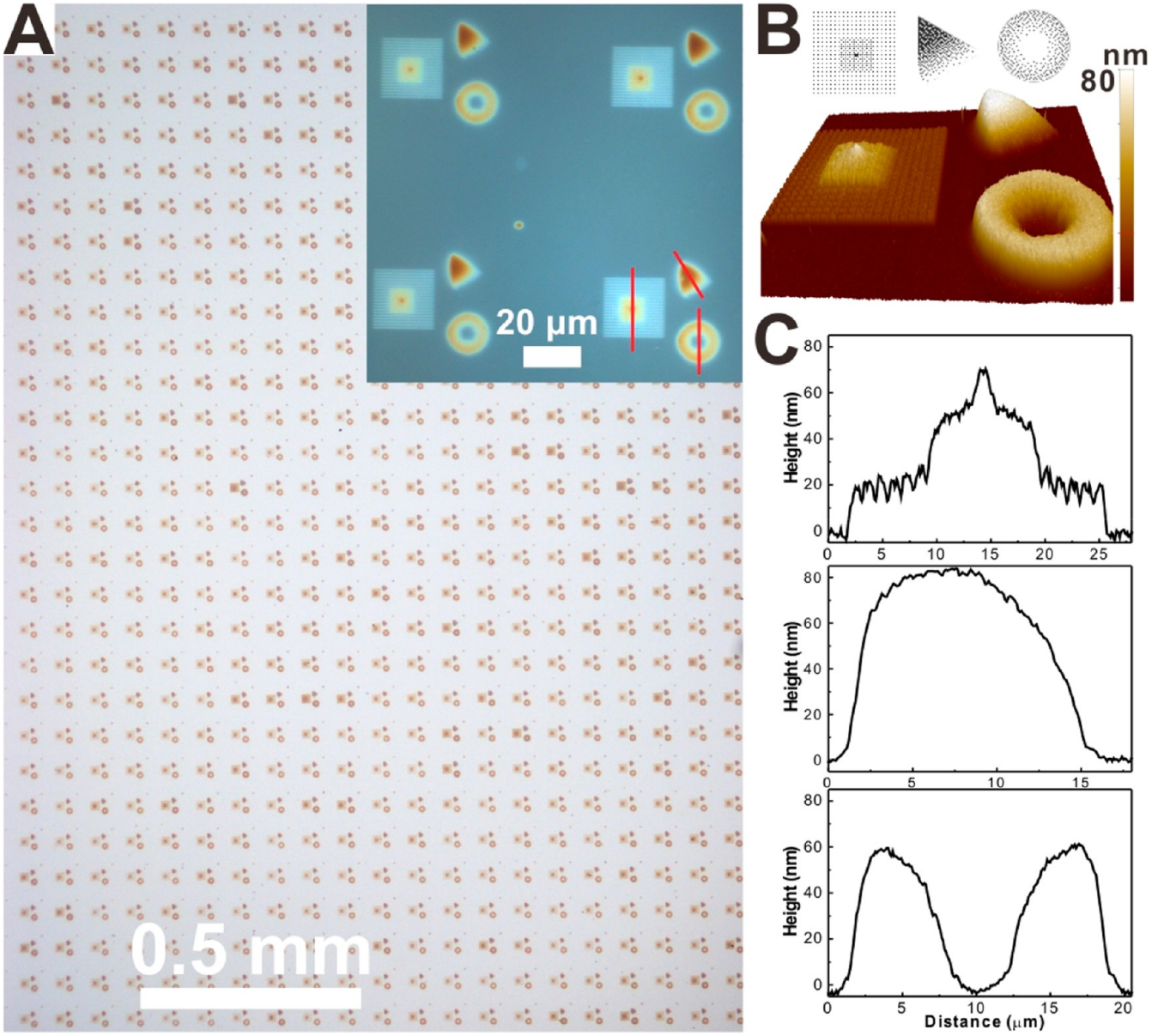

Figure 2. (A) Optical microscope images of the large-area patterned 3D structures of PGMA brushes. The inset shows a magnified polarized optical image of the 3D patterns. (B) The bitmap density maps used to fabricate the 3D structures and the corresponding 3D AFM topography image of the patterned PGMA brushes. (C) Cross-sectional analysis of the topographic profiles of 3D PGMA patterns. The selected cross sectional positions are shown as red lines in the inset of A.

With this principle, we further utilized PPL to fabricate various complex 3D structures of PGMA brushes by converting a grayscale bitmap into a feature density map, in which the black pixels were PPL printing positions while the white pixels served as spacing. Arrays of pyramids, triangular gradients and donuts were chosen as proof-of-concept structures for demonstration (Figure 2). Take the fabrication of pyramids for example. The neighboring black pixels were set respectively to be 1200, 600, and 300 nm for the bottom, middle, and upper layers, corresponding to the resulted brush height of 20, 50, and 70 nm, approximately. The brush height is larger than that of 1D lines shown in Figure 1G, indicating that the dimensionality of pattern also affect the 3D topography. The 2D initiator map for fabricating pyramid leads to enhanced steric repulsion effect from all directions along the 2D plane as well as increased initiator density compared with 1D pattern, and thus much higher brushes with similar feature distance. Again, the 3D patterns appear to be uniform over the writing areas with well controlled height variations of the structures, except for a few arrays showing much higher brushes due to the low-quality tips or nonuniform inking by spin coating.

PGMA Brushes as Resist for Micro/nanofabrication. The as-made large-area, arbitrarily patterned 2D and 3D PGMA brushes can be readily used as functional templates for a wide range of research areas. We demonstrate herein four examples of how one can make use of these PPL-patterned brushes in applications ranging from micro/nanofabrication to bioassays. First of all, we show that patterned PGMA brushes can be used as etching resist in micro/nanofabrication of 2D Au arrays (Figure 3A). Previously, polymer brushes have been reported as superior etching resist to self-assembled monolayers (SAMs) because they are less likely to generate pinholes.[51] As a

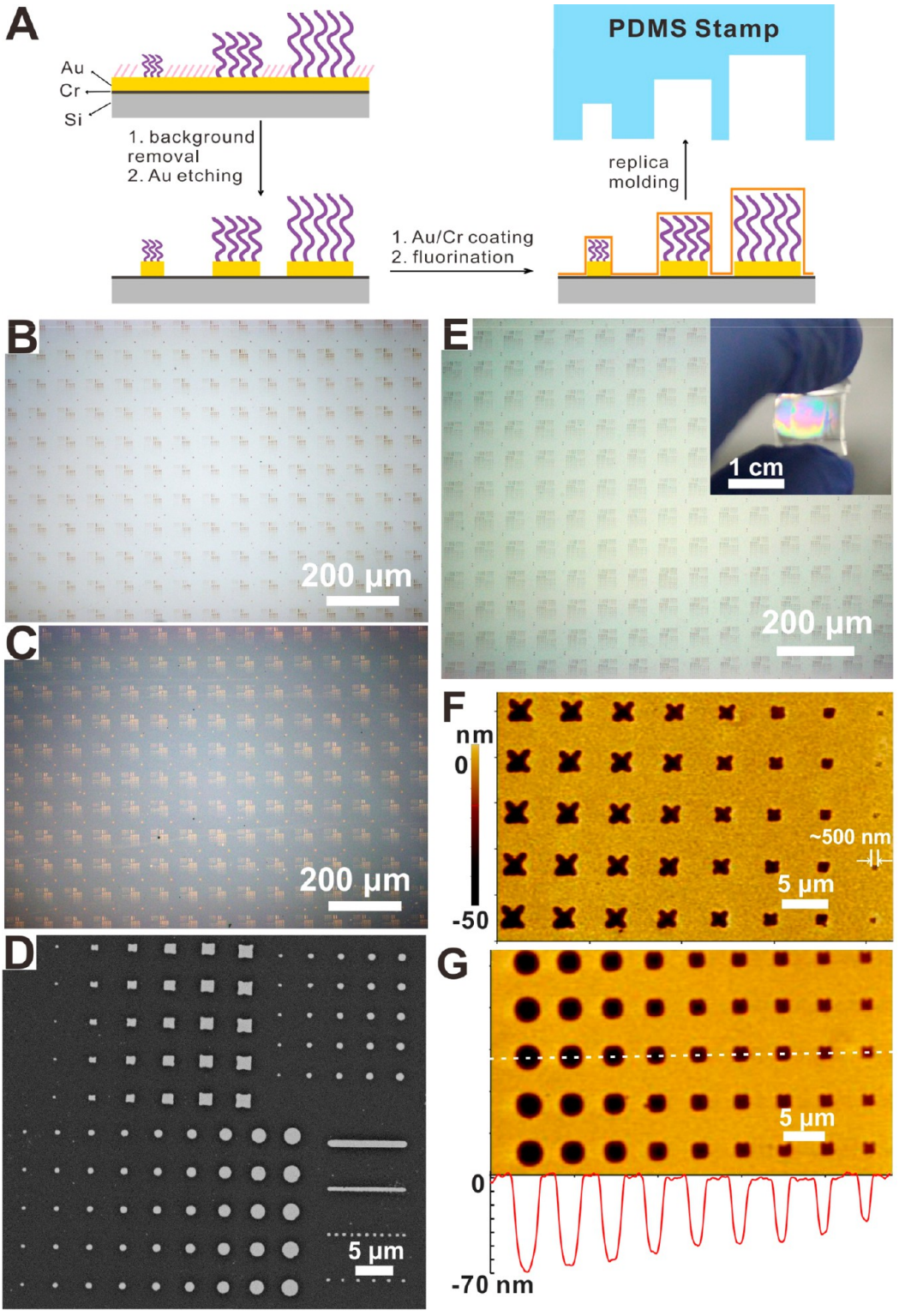

Figure 3. PGMA brushes as resists for micro/nanofabrication. (A) Scheme of the fabrication of Au arrays and PDMS stamp. (B) Optical microscope images of the PPL-patterned PGMA brushes, and (C) the resulted Au arrays after etching. (D) SEM image of a typical array of Au patterns shown in C. (E) Optical microscope image of a PDMS stamp fabricated from patterns shown in C as the mold. The inset shows the digital image of the 1 × 1 cm^2 PDMS stamp. (F, G) AFM topography images of the concave pattern arrays on the PDMS stamp. The profile shows the depth varying from 35 to 70 nm.

demonstration, patterned PGMA brushes on Au made with various z-piezo extensions, dwell times, and feature densities (Figure 3B) were exposed to oxygen plasma briefly to remove the background SAM. The substrate was then immersed in an Au etching solution, in which Au was etched away on the uncovered areas. From the optical microscope and SEM images (Figure 3C and D), it is found that the brush patterns are successfully transferred to Au patterns after the wet etching

dx.doi.org/10.1021/am405555e | *ACS Appl. Mater. Interfaces* 2014, 6, 11955−11964

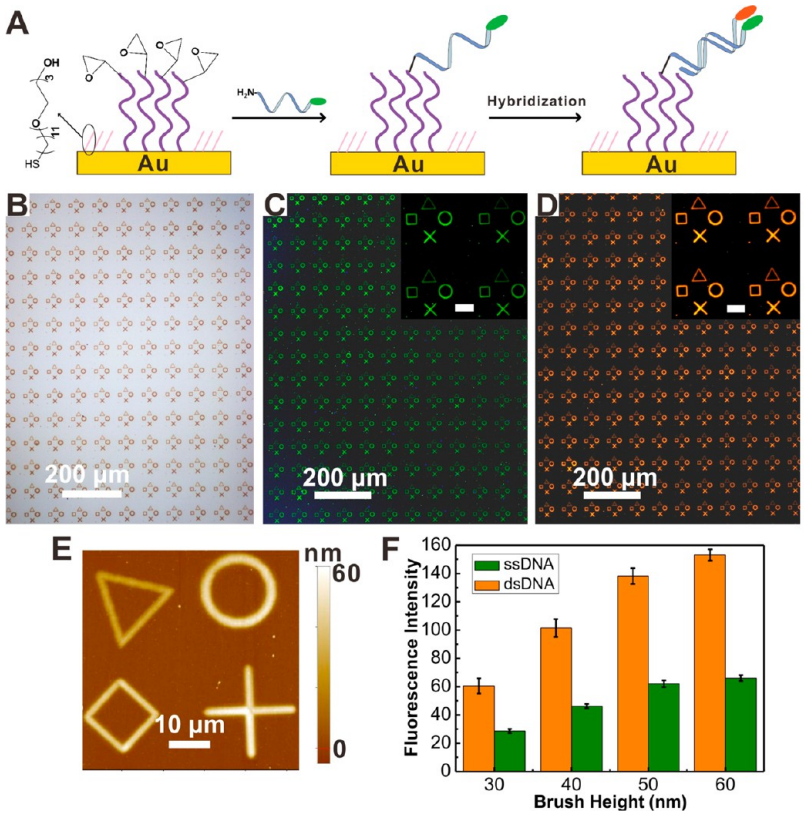

Figure 4. PGMA brushes for DNA immobilization. (A) Scheme of DNA binding and hybridization on PPL-patterned PGMA brushes. (B) Optical microscope image of PGMA brush pattern arrays. (C, D) Fluorescent microscope images of the patterned PGMA brushes bound with 5′-NH_2, 3′-TET-modified ssDNA (C), and after hybridization with 5′-TAMRA-labeled complementary probes (D). λ_{ex} = 465−495 nm, λ_{obs} = 515−555 nm for green fluorescence and λ_{ex} = 528−553 nm, λ_{obs} = 577−632 nm for orange fluorescence. The scale bars in the insets are 20 μm. (E) AFM topography of the patterned PGMA brushes, the approximate height being 30, 40, 50, and 60 nm for triangle, square, ring, and cross, respectively. (F) Statistical results of fluorescence intensity counts for TET-ssDNA and dsDNA with different brush height, obtained from randomly selected 9 arrays.

step. Submicrometer Au features are obtained when PGMA brushes were fabricated under the condition of z-piezo extension < 1 μm and dwell time < 1 s, with the smallest dot diameter of ∼250 nm and line width of ∼450 nm. Note that Au lines are formed only with sufficient polymer brush height, for example, at feature distance of 500 nm or less, otherwise isolated dots are obtained.

These brush-protected Au patterns can further work as hard molds to replicate PDMS stamps for soft lithography. We first coated the Au-etched substrate with a thin Au/Cr layer (10 nm Au/2 nm Cr) followed by surface fluorination treatment with 1H,1H,2H,2H-perfluorodecanethiol. The treated substrate was then used as a mold for PDMS replication to obtain a PDMS stamp with 3D relief structures (Figure 3A and E). The AFM topography images of the PDMS stamp show concave patterns with varying size and depth complementary to the original convex patterns of PGMA brush/Au. The depth of 35−70 nm is in accordance with the total height of PGMA brushes (15−50 nm) and Au (20 nm). Submicrometer features down to ∼500 nm can be successfully replicated.

PGMA Brush Templates for Biomolecular Immobilization. Not only can polymer brushes be used as physical resists for etching and molding purposes but also they act as chemically and biologically active templates if one designs the chemical structures properly. For instance, epoxy groups in PGMA brushes easily react with amines so that one can use them to immobilize biomolecules such as DNAs, proteins, and enzymes.[11] Apart from 2D arrays, 3D biomolecular arrays are particularly interesting platforms for cellular environment since they provides patterned surface with biological/chemical and topographic gradients, which can decouple the complex chemical and physical parameters involved in the cell adhesion and growth processes, such as geometry and nanoscale topography. Also, gradient structures can serve as model systems to understand the transport and motion of biomolecules on the surface.[7,24] We demonstrate herein that the usage of PPL-patterned PGMA brushes for the fabrication of DNA oligonucleotide microarrays and 3D gradient arrays of proteins over large areas. It is worth noting that once being made, PGMA brushes are highly stable at ambient conditions so that they are active even after storage for a few months, providing benefits for practical biochip applications.[52]

For DNA oligonucleotide arrays (Figure 4A), we first fabricated PGMA brushes with EG_3 SAM background by PPL, using four basic pattern designs, namely triangle, square, ring, and cross, as shown in Figure 4B and E. The line width for the four patterns ranged from 1.7 to 2.4 μm and the height was controlled as 30, 40, 50, and 60 nm by tuning the feature distance. A drop of 10 μM solution of 5′-amino-modified, 3′-TET-labeled oligonucleotides (TET-ssDNA) was then dropped onto the patterned PGMA brushes followed by incubation overnight, during which TET-ssDNA covalently bound to the brushes through the ring-opening reaction of epoxy groups. After rinsing away the physisorbed molecules, green fluorescence was seen from the patterned regions under blue light excitation (λ_{ex} = 465−495 nm, λ_{obs} = 515−555 nm), and

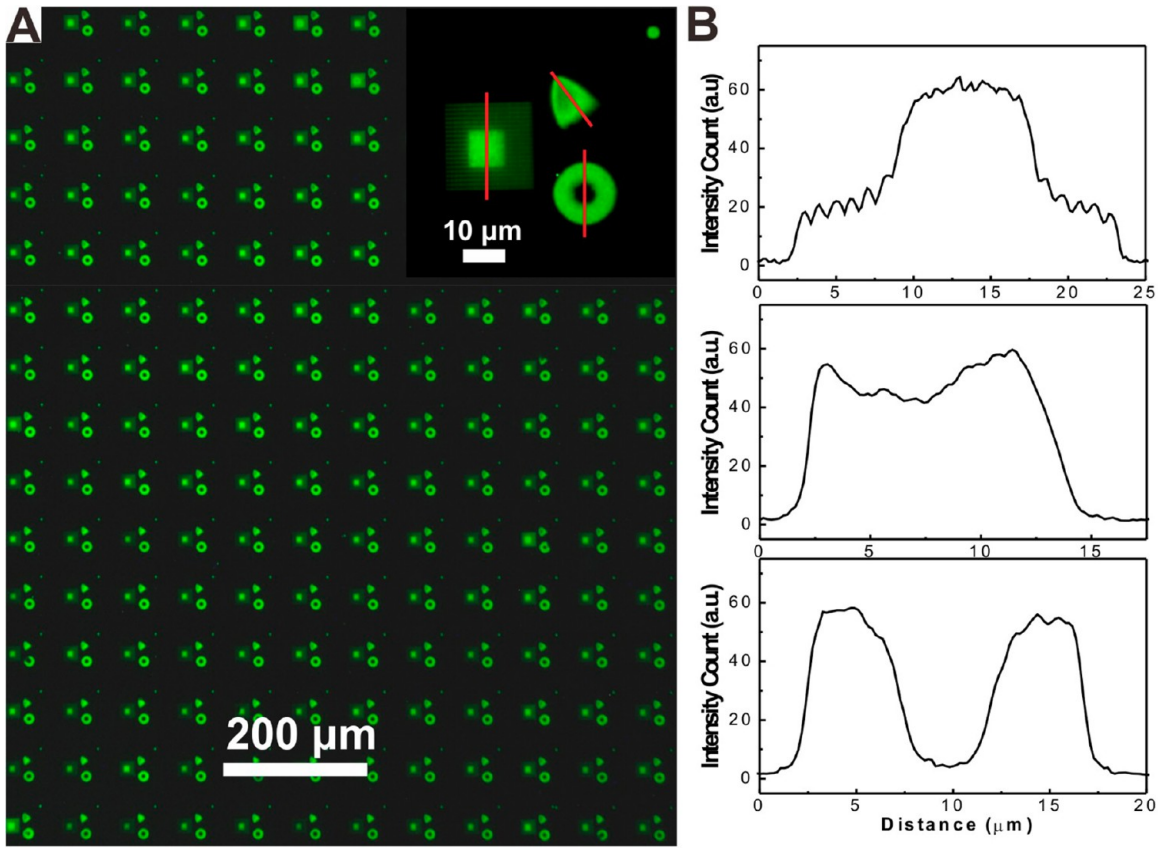

Figure 5. Protein immobilization on 3D-patterned PGMA brushes. (A) Fluorescent microscope images of the immobilized human IgG/FTIC-labeled antihuman IgG on the 3D-patterned PGMA brushes. (B) Cross-sectional analysis of the fluorescence intensity from one array shown in the inset of A.

there was no observable adsorption on the background (Figure 4C). Note that a difference in the fluorescence intensity was observed from four patterns with different brush heights. From statistical results of 9 arrays, the average fluorescence intensity shows significant increase with the increasing brush height from 30 to 50 nm, however, the increment lowers at a brush height of 60 nm (Figure 4F). The PGMA-bound TET-ssDNA was further hybridized with its complementary strand by immersing the substrate into a 100 nM 5′-TAMRA-labeled complementary DNA oligonucleotide (TAMRA-cDNA) solution for 7 h at 45 °C. The success of hybridization was confirmed by the observation of orange fluorescence under green light excitation (λ_{ex} = 528−553 nm, λ_{obs} = 577−632 nm) as well as the decreased intensity in green fluorescence under blue excitation due to the fluorescence resonance energy transfer process between the two adjacent dyes (Figure 4D and SI, Figure S4).[53] As a control experiment, we tested a random sequenced probe and observed none of the two above phenomena. The double-stranded DNA also shows stronger fluorescence on the higher brushes.

For the fabrication of 3D protein arrays, we used human IgG and antihuman IgG as demonstration. Human IgG was first immobilized onto the above-mentioned 3D brush structures (as those shown in Figure 2) by incubating the brush-patterned substrate with a 50 μg mL^{-1} IgG solution at room temperature for 16 h. After passivating with bovine serum albumins (BSA) and washing, the substrate was then covered with FITC-labeled antihuman IgG (50 μg mL^{-1}) and incubated for 2 h. The specific biomolecular interaction between the immobilized IgG and the captured anti-IgG resulted in strong fluorescence (Figure 5). The obtained protein microarrays exhibit gradient fluorescence intensity as a function of its corresponding topography (as those shown in Figure 2B). When the brush height is below 60 nm, the fluorescence intensity increases as brush height increases, and it reaches a plateau when the brush height is around 60 nm. Surprisingly, the fluorescence intensity decreases when the brush is higher than ∼65 nm. This phenomenon may be attributed to the difficulty in infiltration into polymer brushes with very high grafting density for antihuman IgG.[54,55] The results suggest that 3D polymer brushes are potentially effective platforms to examine the infiltration of molecules or even nanomaterials into polymer of different grafting densities.

4. CONCLUSIONS

We have demonstrated the first example of large area (∼2 cm^2) serial patterning of complex 2D and 3D polymer brushes by polymer pen lithography (PPL) and SI-ATRP. Importantly, the throughput of fabrication is 3 orders of magnitude higher than the best results reported previously using serial lithographic methods. The shape, feature size, and height of the fabricated brush patterns are well-controlled by varying the dwell time, contact force and feature distance, with good uniformity. On one hand, the patterned PGMA brushes were demonstrated as effective etching resists for fabricating Au micro/nanostructures and hard molds for replicating centimeter-sized PDMS stamps. On the other hand, PGMA brush templates were also used as robust active platforms for immobilization of biomolecules such

as DNA and proteins to produce biochips. This low-cost "bench-top" fabrication tool meets the requirements for lab-scale high speed prototyping of micrometer and submicrometer structures and proof-of-concept experiments. It shall have remarkable application potential for scientists and engineers in chemical, material, and biomedical research fields, considering that polymer brushes possess a wide diversity of tailored functionality, for example, templates for loading ions and nanoparticles or guiding self-assembly, and responsive properties to environmental stimuli, etc. In addition, the resolution and the uniformity of fabrication can be enhanced, in principle, by using high quality tip arrays with sharper and well-engineered tip structures.[56−59]

■ ASSOCIATED CONTENT

Supporting Information

Images of centimeter-area patterned brush arrays, ATR-IR spectroscopic analysis of PGMA brushes and control experiment results on oligonucleotide hybridization. This material is available free of charge via the Internet at http://pubs.acs.org.

■ AUTHOR INFORMATION

Corresponding Author

*Fax: (+) 852-27731432. E-mail: tczzheng@polyu.edu.hk.

Notes

The authors declare no competing financial interest.

■ ACKNOWLEDGMENTS

Z.J.Z. acknowledges National Natural Science Foundation of China (Project 51273167) and General Research Fund of Hong Kong (Project PolyU5041/11P) for financial support of this work. The authors acknowledge Prof. Hongwei Ma in Suzhou Institute of Nano-Tech and Nano-Bionics (SINANO), CAS for providing the ATRP initiators, Prof. Xingyu Jiang in National Center for Nanoscience and Technology, China, for providing the EG_3 thiol, Jingjing Wei in The Chinese University of Hong Kong for the help in monomer purification.

■ REFERENCES

(1) Nie, Z. H.; Kumacheva, E. Patterning surfaces with functional polymers. *Nat. Mater.* **2008**, *7*, 277−290.

(2) Stuart, M. A. C.; Huck, W. T. S.; Genzer, J.; Muller, M.; Ober, C.; Stamm, M.; Sukhorukov, G. B.; Szleifer, I.; Tsukruk, V. V.; Urban, M.; Winnik, F.; Zauscher, S.; Luzinov, I.; Minko, S. Emerging applications of stimuli-responsive polymer materials. *Nat. Mater.* **2010**, *9*, 101−113.

(3) Zhou, X. Z.; Boey, F.; Huo, F. W.; Huang, L.; Zhang, H. Chemically functionalized surface patterning. *Small* **2011**, *7*, 2273−2289.

(4) Bettinger, C. J.; Langer, R.; Borenstein, J. T. Engineering substrate topography at the micro- and nanoscale to control cell function. *Angew. Chem., Int. Ed.* **2009**, *48*, 5406−5415.

(5) Mager, M. D.; LaPointe, V.; Stevens, M. M. Exploring and exploiting chemistry at the cell surface. *Nat. Chem.* **2011**, *3*, 582−589.

(6) Barbey, R.; Lavanant, L.; Paripovic, D.; Schuwer, N.; Sugnaux, C.; Tugulu, S.; Klok, H. A. Polymer brushes via surface-initiated controlled radical polymerization: Synthesis, characterization, properties, and applications. *Chem. Rev.* **2009**, *109*, 5437−5527.

(7) Zhou, X. C.; Liu, X. Q.; Xie, Z.; Zheng, Z. J. 3D-patterned polymer brush surfaces. *Nanoscale* **2011**, *3*, 4929−4939.

(8) Pirri, G.; Chiari, M.; Damin, F.; Meo, A. Microarray glass slides coated with block copolymer brushes obtained by reversible addition chain-transfer polymerization. *Anal. Chem.* **2006**, *78*, 3118−3124.

(9) Barbey, R.; Kauffmann, E.; Ehrat, M.; Klok, H. A. Protein microarrays based on polymer brushes prepared via surface-initiated atom transfer radical polymerization. *Biomacromolecules* **2010**, *11*, 3467−3479.

(10) Hucknall, A.; Kim, D.-H.; Rangarajan, S.; Hill, R. T.; Reichert, W. M.; Chilkoti, A. Simple fabrication of antibody microarrays on nonfouling polymer brushes with femtomolar sensitivity for protein analytes in serum and blood. *Adv. Mater.* **2009**, *21*, 1968−1971.

(11) Jiang, H.; Xu, F. J. Biomolecule-functionalized polymer brushes. *Chem. Soc. Rev.* **2013**, *42*, 3394−3426.

(12) Ma, H. W.; Hyun, J. H.; Stiller, P.; Chilkoti, A. "Non-fouling" oligo(ethylene glycol)-functionalized polymer brushes synthesized by surface-initiated atom transfer radical polymerization. *Adv. Mater.* **2004**, *16*, 338−341.

(13) Bernards, M. T.; Cheng, G.; Zhang, Z.; Chen, S. F.; Jiang, S. Y. Nonfouling polymer brushes via surface-initiated, two-component atom transfer radical polymerization. *Macromolecules* **2008**, *41*, 4216−4219.

(14) Liu, X. Q.; Chang, H. X.; Li, Y.; Huck, W. T. S.; Zheng, Z. J. Polyelectrolyte-bridged metal/cotton hierarchical structures for highly durable conductive yarns. *ACS Appl. Mater. Interfaces* **2010**, *2*, 529−535.

(15) Garcia, A.; Polesel-Maris, J.; Viel, P.; Palacin, S.; Berthelot, T. Localized ligand induced electroless plating (LIEP) process for the fabrication of copper patterns onto flexible polymer substrates. *Adv. Funct. Mater.* **2011**, *21*, 2096−2102.

(16) Tokarev, I.; Tokareva, I.; Minko, S. Optical nanosensor platform operating in near-physiological ph range via polymer-brush-mediated plasmon coupling. *ACS Appl. Mater. Interfaces* **2011**, *3*, 143−146.

(17) Chen, T.; Chang, D. P.; Zhang, J. M.; Jordan, R.; Zauscher, S. Manipulating the motion of gold aggregates using stimulus-responsive patterned polymer brushes as a motor. *Adv. Funct. Mater.* **2012**, *22*, 429−434.

(18) Tan, K. Y.; Hughes, T. L.; Nagl, M.; Huck, W. T. S. Nonfouling capture-release substrates based on polymer brushes for separation of water-dispersed oil droplets. *ACS Appl. Mater. Interfaces* **2012**, *4*, 6403−6409.

(19) Olivier, A.; Meyer, F.; Raquez, J. M.; Damman, P.; Dubois, P. Surface-initiated controlled polymerization as a convenient method for designing functional polymer brushes: From self-assembled monolayers to patterned surfaces. *Prog. Polym. Sci.* **2012**, *37*, 157−181.

(20) Chen, T.; Amin, I.; Jordan, R. Patterned polymer brushes. *Chem. Soc. Rev.* **2012**, *41*, 3280−3296.

(21) Chen, J. K.; Pai, P. C.; Chang, J. Y.; Fan, S. K. pH-Responsive one-dimensional periodic relief grating of polymer brush-gold nanoassemblies on silicon surface. *ACS Appl. Mater. Interfaces* **2012**, *4*, 1935−1947.

(22) Li, Y. F.; Zhang, J. H.; Liu, W. D.; Li, D. W.; Fang, L. P.; Sun, H. C.; Yang, B. Hierarchical polymer brush nanoarrays: A versatile way to prepare multiscale patterns of proteins. *ACS Appl. Mater. Interfaces* **2013**, *5*, 2126−2132.

(23) Yu, Q.; Cho, J.; Shivapooja, P.; Ista, L. K.; Lopez, G. P. Nanopatterned smart polymer surfaces for controlled attachment, killing, and release of bacteria. *ACS Appl. Mater. Interfaces* **2013**, *5*, 9295−9304.

(24) Lin, X. K.; He, Q.; Li, J. B. Complex polymer brush gradients based on nanolithography and surface-initiated polymerization. *Chem. Soc. Rev.* **2012**, *41*, 3584−3593.

(25) He, Q.; Kueller, A.; Schilp, S.; Leisten, F.; Kolb, H.-A.; Grunze, M.; Li, J. Fabrication of controlled thermosensitive polymer nanopatterns with one-pot polymerization through chemical lithography. *Small* **2007**, *3*, 1860−1865.

(26) Schilp, S.; Ballav, N.; Zharnikov, M. Fabrication of a full-coverage polymer nanobrush on an electron-beam-activated template. *Angew. Chem., Int. Ed.* **2008**, *47*, 6786−6789.

(27) Steenackers, M.; Jordan, R.; Kuller, A.; Grunze, M. Engineered polymer brushes by carbon templating. *Adv. Mater.* **2009**, *21*, 2921−2925.

(28) Paik, M. Y.; Xu, Y. Y.; Rastogi, A.; Tanaka, M.; Yi, Y.; Ober, C. K. Patterning of polymer brushes. A direct approach to complex, subsurface structures. *Nano Lett.* **2010**, *10*, 3873−3879.

(29) Liu, X. G.; Guo, S. W.; Mirkin, C. A. Surface and site-specific ring-opening metathesis polymerization initiated by dip-pen nanolithography. *Angew. Chem., Int. Ed.* **2003**, *42*, 4785−4789.
(30) Hirtz, M.; Brinks, M. K.; Miele, S.; Studer, A.; Fuchs, H.; Chi, L. F. Structured polymer brushes by AFM lithography. *Small* **2009**, *5*, 919−923.
(31) Liu, X.; Li, Y.; Zheng, Z. Programming nanostructures of polymer brushes by dip-pen nanodisplacement lithography (DNL). *Nanoscale* **2010**, *2*, 2614−2618.
(32) Zhou, X. C.; Wang, X. L.; Shen, Y. D.; Xie, Z.; Zheng, Z. J. Fabrication of arbitrary three-dimensional polymer structures by rational control of the spacing between nanobrushes. *Angew. Chem., Int. Ed.* **2011**, *50*, 6506−6510.
(33) Zhou, X. C.; Liu, Z. L.; Xie, Z.; Liu, X. Q.; Zheng, Z. J. High-resolution, large-area, serial fabrication of 3D polymer brush structures by parallel dip-pen nanodisplacement lithography. *Small* **2012**, *8*, 3568−3572.
(34) Gan, T.; Zhou, X.; Ma, C.; Liu, X.; Xie, Z.; Zhang, G.; Zheng, Z. Liquid-mediated three-dimensional scanning probe nanosculpting. *Small* **2013**, *9*, 2851−2856.
(35) Xie, Z.; Zhou, X. C.; Tao, X. M.; Zheng, Z. J. Polymer nanostructures made by scanning probe lithography: Recent progress in material applications. *Macromol. Rapid Commun.* **2012**, *33*, 359−373.
(36) Schuh, C.; Santer, S.; Prucker, O.; Ruhe, J. Polymer brushes with nanometer-scale gradients. *Adv. Mater.* **2009**, *21*, 4706−4710.
(37) Poelma, J. E.; Fors, B. P.; Meyers, G. F.; Kramer, J. W.; Hawker, C. J. Fabrication of complex three-dimensional polymer brush nanostructures through light-mediated living radical polymerization. *Angew. Chem., Int. Ed.* **2013**, *52*, 6844−6848.
(38) Fors, B. P.; Poelma, J. E.; Menyo, M. S.; Robb, M. J.; Spokoyny, D. M.; Kramer, J. W.; Waite, J. H.; Hawker, C. J. Fabrication of unique chemical patterns and concentration gradients with visible light. *J. Am. Chem. Soc.* **2013**, *135*, 14106−14109.
(39) Steenackers, M.; Gigler, A. M.; Zhang, N.; Deubel, F.; Seifert, M.; Hess, L. H.; Lim, C. H. Y. X.; Loh, K. P.; Garrido, J. A.; Jordan, R.; Stutzmann, M.; Sharp, I. D. Polymer brushes on graphene. *J. Am. Chem. Soc.* **2011**, *133*, 10490−10498.
(40) Benetti, E. M.; Acikgoz, C.; Sui, X.; Vratzov, B.; Hempenius, M. A.; Huskens, J.; Vancso, G. J. Nanostructured polymer brushes by UV-assisted imprint lithography and surface-initiated polymerization for biological functions. *Adv. Funct. Mater.* **2011**, *21*, 2088−2095.
(41) Moran, I. W.; Ell, J. R.; Carter, K. R. Functionally decoupled soft lithography for patterning polymer brushes. *Small* **2011**, *7*, 2669−2674.
(42) Wang, M.; Comrie, J. E.; Bai, Y. P.; He, X. M.; Guo, S. Y.; Huck, W. T. S. Formation of hierarchically structured thin films. *Adv. Funct. Mater.* **2009**, *19*, 2236−2243.
(43) Chen, T.; Zhong, J. M.; Chang, D. P.; Carcia, A.; Zauscher, S. Fabrication of micropatterned stimulus-responsive polymer-brush 'anemone'. *Adv. Mater.* **2009**, *21*, 1825−1829.
(44) Chen, T.; Jordan, R.; Zauscher, S. Dynamic microcontact printing for patterning polymer-brush microstructures. *Small* **2011**, *7*, 2148−2152.
(45) Gao, T. T.; Wang, X. L.; Yu, B.; Wei, Q. B.; Xia, Y. Q.; Zhou, F. Noncovalent microcontact printing for grafting patterned polymer brushes on graphene films. *Langmuir* **2013**, *29*, 1054−1060.
(46) Huo, F. W.; Zheng, Z. J.; Zheng, G. F.; Giam, L. R.; Zhang, H.; Mirkin, C. A. Polymer pen lithography. *Science* **2008**, *321*, 1658−1660.
(47) Zheng, Z. J.; Daniel, W. L.; Giam, L. R.; Huo, F. W.; Senesi, A. J.; Zheng, G. F.; Mirkin, C. A. Multiplexed protein arrays enabled by polymer pen lithography: Addressing the inking challenge. *Angew. Chem., Int. Ed.* **2009**, *48*, 7626−7629.
(48) Liao, X.; Braunschweig, A. B.; Zheng, Z. J.; Mirkin, C. A. Force- and time-dependent feature size and shape control in molecular printing via polymer-pen lithography. *Small* **2010**, *6*, 1082−1086.
(49) Chai, J. A.; Huo, F. W.; Zheng, Z. J.; Giam, L. R.; Shim, W.; Mirkin, C. A. Scanning probe block copolymer lithography. *Proc. Natl. Acad. Sci. U.S.A.* **2010**, *107*, 20202−20206.
(50) Giam, L. R.; Massich, M. D.; Hao, L.; Wong, L. S.; Mader, C. C.; Mirkin, C. A. Scanning probe-enabled nanocombinatorics define the relationship between fibronectin feature size and stem cell fate. *Proc. Natl. Acad. Sci. U.S.A.* **2012**, *109*, 4377−4382.
(51) Shah, R. R.; Merreceyes, D.; Husemann, M.; Rees, I.; Abbott, N. L.; Hawker, C. J.; Hedrick, J. L. Using atom transfer radical polymerization to amplify monolayers of initiators patterned by microcontact printing into polymer brushes for pattern transfer. *Macromolecules* **2000**, *33*, 597−605.
(52) Jang, J.-W.; Collins, J. M.; Nettikadan, S. User-friendly universal and durable subcellular-scaled template for protein binding: Application to single-cell patterning. *Adv. Funct. Mater.* **2013**, *23*, 5840−5845.
(53) Yea, K. H.; Lee, S.; Choo, J.; Oh, C. H.; Lee, S. Fast and sensitive analysis of DNA hybridization in a PDMS micro-fluidic channel using fluorescence resonance energy transfer. *Chem. Commun.* **2006**, 1509−1511.
(54) Rahim, F. A.; Dong-Hwan, K. Physical immobilization of antibodies in densely grafted polymer brushes via spot-drying: towards optimal protein loading. *RSC Adv.* **2013**, *3*, 9785−9793.
(55) Akkahat, P.; Mekboonsonglarp, W.; Kiatkamjornwong, S.; Hoven, V. P. Surface-grafted poly(acrylic acid) brushes as a precursor layer for biosensing applications: Effect of graft density and swellability on the detection efficiency. *Langmuir* **2012**, *28*, 5302−5311.
(56) Huo, F. W.; Zheng, G. F.; Liao, X.; Giam, L. R.; Chai, J. A.; Chen, X. D.; Shim, W. Y.; Mirkin, C. A. Beam pen lithography. *Nat. Nanotechnol.* **2010**, *5*, 637−640.
(57) Shim, W.; Braunschweig, A. B.; Liao, X.; Chai, J.; Lim, J. K.; Zheng, G.; Mirkin, C. A. Hard-tip, soft-spring lithography. *Nature* **2011**, *469*, 516−521.
(58) Xie, Z.; Shen, Y. D.; Zhou, X. C.; Yang, Y.; Tang, Q.; Miao, Q.; Su, J.; Wu, H. K.; Zheng, Z. J. Polymer pen lithography using dual-elastomer tip arrays. *Small* **2012**, *8*, 2664−2669.
(59) Zhong, X.; Bailey, N. A.; Schesing, K. B.; Bian, S. D.; Campos, L. M.; Braunschweig, A. B. Materials for the preparation of polymer pen lithography tip arrays and a comparison of their printing properties. *J. Polym. Sci., Part A: Polym. Chem.* **2013**, *51*, 1533−1539.